

# Criticality of rumor propagation on small-world networks

Damián H. Zanette

*Consejo Nacional de Investigaciones Científicas y Técnicas  
Centro Atómico Bariloche and Instituto Balseiro, 8400 Bariloche, Río Negro, Argentina*  
(October 29, 2018)

We show that a simple model for the propagation of a rumor on a small-world network exhibits critical behavior at a finite randomness of the underlying graph. The transition occurs between a regime where the rumor “dies” in a small neighborhood of its origin, and a regime where it spreads over a finite fraction of the whole population. Critical exponents are evaluated through finite-size scaling analysis, and the dependence of the critical randomness with the network connectivity is studied. The behavior of this system as a function of the network randomness bears noticeable similarities with an epidemiological model reported recently [M. Kuperman and G. Abramson, *Phys. Rev. Lett.* **86**, 2909 (2001)], in spite of substantial differences in the respective dynamical rules.

Small-world networks have been introduced as an interpolation between ordered and random graphs, to capture two specific features of real neural, social, and technological networks [1,2]. On one hand, they have a relatively large clustering coefficient, i.e. the probability that two neighbors of a given vertex are in turn mutual neighbors is high, as in ordered graphs. On the other, the typical separation between two vertices is much smaller than the total number of vertices, as in random graphs. Whereas the geometrical properties of small-world networks have been studied in detail [1–10], less attention has been paid to the dynamical properties resulting from their partially random structure [2,10–12]. As explained in more detail below, the structure of small-world networks is parametrized by the randomness  $p$ , where  $p = 0$  and  $p = 1$  correspond to fully ordered and random networks, respectively. It has been shown that, in asymptotically large small-world networks, statistical geometrical properties—such as the mean distance between vertices—exhibit qualitatively the same behavior for any  $p > 0$ . Here, we study an epidemic-like propagation process on a small-world network which, in contrast with geometrical properties, shows a transition between two qualitatively different dynamical regimes at a finite value of  $p$ . Since this model addresses a social process and small-world networks are a presumably realistic representation of social networks, the analysis could be relevant to the description of threshold phenomena in real societies.

Our model [13,14] consists of an  $N$ -element population where, at each time step, each element adopts one of three possible states. By analogy with epidemiological

SIR models [15], these states are called susceptible (S), infected (I), and refractory (R). The evolution proceeds as follows. At each time step a randomly chosen infected element  $i$  contacts another element  $j$ . Then, (i) if  $j$  is in the susceptible state, it becomes infected; (ii) if, on the contrary,  $j$  is infected or refractory,  $i$  becomes refractory. These rules are better interpreted in the frame of a rumor spreading process, where S-elements have not heard the rumor yet, I-elements have heard the rumor and are willing to transmit it, and R-elements have lost their interest in the rumor and do not transmit it. Initially, only one element is infected and the remaining  $N - 1$  elements are susceptible. During the first stage of the evolution, the number of I-elements increases. Since this also implies a growth of the R-population, the contacts of I-elements between themselves and with R-elements become more frequent. After a while, in consequence, the I-population begins to decline. Eventually, it vanishes and the evolution stops. At the end,  $N_R$  elements—now in the refractory state—have been infected at some stage during the evolution. Numerical simulations and analytical results show that, generally,  $N_R < N$ . Therefore, there is a fraction of the population that never hears the rumor. In the original version of this model, each I-element is allowed to contact at random any other element of the population. It has been proven that, in such situation, the ratio  $N_R/N$  approaches a well-defined limit,  $N_R/N = 0.796\dots$ , for asymptotically large values of  $N$  [16,17].

Here, in contrast, we assume that the elements are situated at the vertices of a small-world network, and contacts can be established between linked elements only. The small-world network is constructed from a one-dimensional ordered network with periodic boundary conditions—a ring—where each node is linked to its  $2K$  nearest neighbors, i.e. to the  $K$  nearest neighbors clockwise and counterclockwise [1,2,12]. Then, each of the  $K$  clockwise connections of each node  $i$  is rewired with probability  $p$  to a randomly chosen node  $j$ , not belonging to the neighborhood of  $i$ . A short-cut between two otherwise distant regions is thus created. Double and multiple links are forbidden, and realizations where the small-world network becomes disconnected are discarded. As advanced above, the parameter  $p$  measures the randomness of the resulting small-world network. Note that, independently of the value of  $p$ , the average number of links per site is always  $2K$ . We have performed series of  $10^3$  to  $10^5$  numerical realizations of the model for several values of  $p$ ,  $N$ , and  $K$ . At each realization, the small-

world network was generated anew and the evolution was recorded until the exhaustion of the population

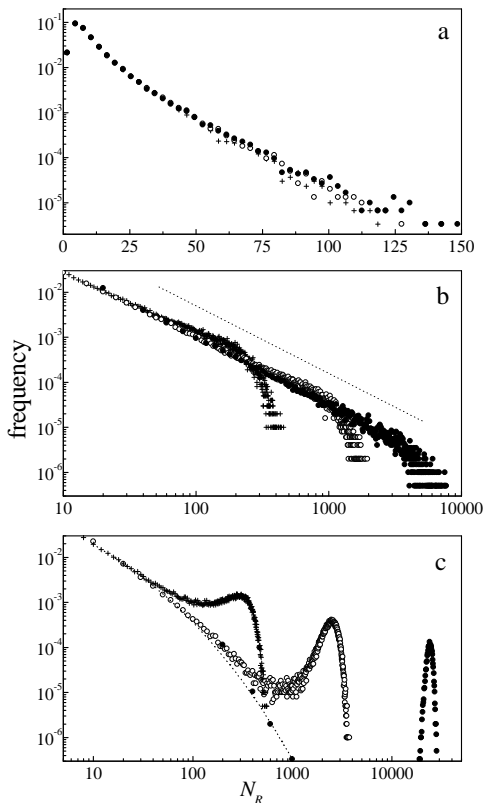


FIG. 1. Frequency distribution of the number  $N_R$  of R-elements at the end of the evolution, for  $K = 2$  and (a)  $p = 0.05$ , (b)  $p = 0.19$ , and (c)  $p = 0.3$ . Different symbols correspond to  $N = 10^3$  (crosses),  $N = 10^4$  (empty dots), and  $N = 10^5$  (full dots). In (b), the dotted straight line has slope  $-1.5$ . The dotted curve in (c) is a schematic representation of the  $N$ -independent profile observed for small  $N_R$ . Note carefully the different scales of the three plots.

In the first place, we have studied the distribution of the number  $N_R$  of R-elements at the end of the evolution for  $K = 2$ . Figure 1 shows the normalized frequency  $f(N_R)$  obtained from series of  $10^5$  realizations for selected values of  $p$  and  $N$ . For small randomness ( $p = 0.05$ , Fig. 1a) the distribution is approximately exponential and does not depend on  $N$ . In this regime, the rumor “dies” after a few time steps in a small neighborhood of its origin, due to the loss of interest of the highly interconnected elements close to the initially infected site. Therefore, the size  $N$  of the whole population is irrelevant to the value of  $N_R$ . The situation is considerably different for relatively large randomness ( $p = 0.3$ , Fig. 1c). Here the distribution  $f(N_R)$  is bimodal, with a maximum close to  $N_R = 0$  (not shown in the figure) and an additional bump for larger  $N_R$ . Near  $N_R = 0$ , the frequency is independent of  $N$ , as in the case of small

randomness. Contributions to this zone of the distribution come from realizations where propagation ceases before a short-cut is reached. In contrast, the additional structure is strongly dependent on  $N$ . The position of its maximum, in fact, grows linearly, as  $N_R^{\max} \approx 0.25N$ . In a typical realization contributing to this zone of the distribution, many contacts occur through short-cuts and a finite portion of the population becomes infected. The intermediate regime, just before the large- $N_R$  structure begins to build up, is illustrated in Fig. 1b for  $p = 0.19$ . The frequency follows here a power law,  $f(N_R) \sim N_R^{-\alpha}$  with  $\alpha \approx 1.5$ , over a substantial interval. This interval is limited by above by a smooth cut-off, which shifts to larger values of  $N_R$  as  $N^\beta$ , with  $\beta \sim 0.5$ .

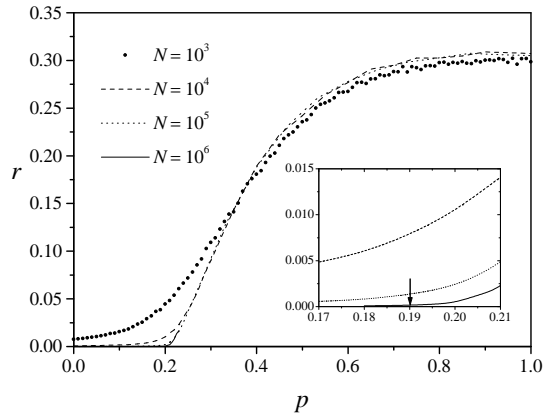


FIG. 2. Average fraction  $r = \langle N_R/N \rangle$  of refractory elements at the end of the evolution as a function of the randomness  $p$  on a small-world network with  $K = 2$ , and for  $N = 10^3$  (dots),  $N = 10^4$  (dashed line),  $N = 10^5$  (dotted line), and  $N = 10^6$  (full line). The insert shows a close-up in the transition zone. The arrow indicates the critical value of  $p$ , determined as explained in the text.

The appearance of a well-defined power-law distribution is a clue to the critical-phenomenon nature of the transition from the regime where the rumor remains localized to the regime where it spreads over a finite fraction of the population. To characterize the transition, we choose as an order parameter the average fraction  $N_R/N$  of R-elements at the end of the process,

$$r = \langle N_R/N \rangle = N^{-1} \sum_{N_R=0}^N N_R f(N_R), \quad (1)$$

which can be straightforwardly calculated from the numerical results. In the small-randomness regime, where  $f(N_R)$  is independent of  $N$ , we expect  $r \sim N^{-1}$ , so that  $r \rightarrow 0$  as  $N \rightarrow \infty$ . For large  $p$ , in contrast, the presence of the large- $N_R$  maximum in  $f(N_R)$  should provide a finite contribution to  $r$  even for asymptotically large populations. These features are verified in numerical realizations. Figure 2 shows  $r$  as a function of  $p$ , calculated

in series of  $10^3$  to  $10^4$  realizations for  $N$  ranging from  $10^3$  to  $10^6$  and  $K = 2$ . A well-defined transition at a finite randomness  $p_c \approx 0.2$  is apparent for large  $N$ . The insert of Fig. 2 shows a close-up of the main plot near  $p_c$ . The smoothness of the curves, observed even for the largest values of  $N$ , suggest that the critical exponent  $\gamma$  associated with  $r \sim |p - p_c|^\gamma$  just above the transition, should be larger than unity.

To determine the values of  $p_c$  and  $\gamma$  we apply finite-size scaling analysis [18]. Results are presented in Fig. 3. The insert shows a plot of the fraction  $r$  as a function of  $N$  for several values of the randomness  $p$ . With  $p = 0.17$  and  $0.18$  we find the subcritical behavior expected for  $p < p_c$ , i.e.  $r \sim N^{-1}$ . For  $p = 0.20$  and  $0.21$ , on the other hand,  $r$  saturates to a finite value for very large  $N$ . Between these two regimes, with  $p = 0.19$ ,  $r$  decreases as  $r \sim N^{-\rho}$ , with  $\rho = 0.78 \pm 0.02$ . We identify this intermediate regime with the critical point, and thus get  $p_c = 0.19 \pm 0.01$ .

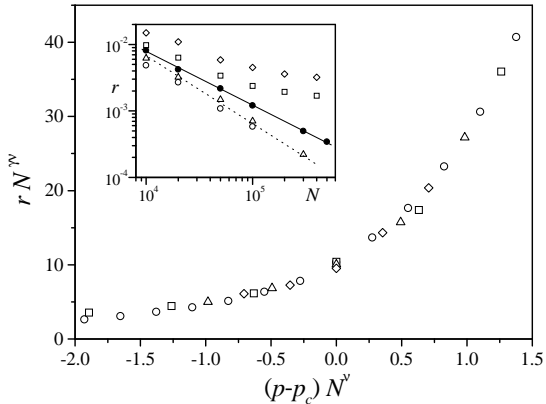


FIG. 3. Data collapse in the finite-size scaling of the fraction  $r$  as a function of  $p - p_c$ , Eq. (2), with  $\nu = 0.36$ . Different symbols correspond to different values of  $N$ , ranging from  $10^4$  to  $10^6$ . The insert shows  $r$  as a function of  $N$  for five values of the randomness: from below,  $p = 0.17, 0.18, 0.19, 0.20$ , and  $0.21$ . The dashed and the full line have slopes  $-1$  and  $-0.78$ , respectively.

Once  $p_c$  has been determined, the critical exponent  $\gamma$  is obtained from the finite-size scaling *Ansatz* [18]

$$rN^{\gamma\nu} = F[(p - p_c)N^\nu]. \quad (2)$$

For  $p = p_c$  we have  $r = F(0)N^{-\gamma\nu}$ , so that  $\gamma\nu = \rho = 0.78 \pm 0.02$ . The best data collapse near the critical point is obtained for  $\nu = 0.36 \pm 0.01$ , as shown in Fig. 3. This yields  $\gamma = 2.2 \pm 0.1$ .

We have examined this model for other values of  $K$ , up to  $K = 10$ , and found the same kind of transition in all cases. The average fraction  $r$  as a function of  $p$  is shown in Figure 4 for  $N = 10^5$  and several values of  $K$ , calculated over  $10^3$  realizations. It is seen that the critical randomness  $p_c$  decreases as  $K$  grows. This is due

to the increment in the number of long-range contacts per element, as a consequence of the higher connectivity of each site. On the other hand, the value of  $r$  at  $p = 1$ ,  $r_1$ , grows with  $K$  and approaches the level expected for the original version of the model,  $r^* = 0.796 \dots$  [16,17]. The insert in Fig. 4 displays the dependence of  $p_c$  and of the difference  $r^* - r_1$  with  $K$ . Though this plot covers less than one order of magnitude in the  $K$ -axis, the results suggest power-law decays for both quantities.

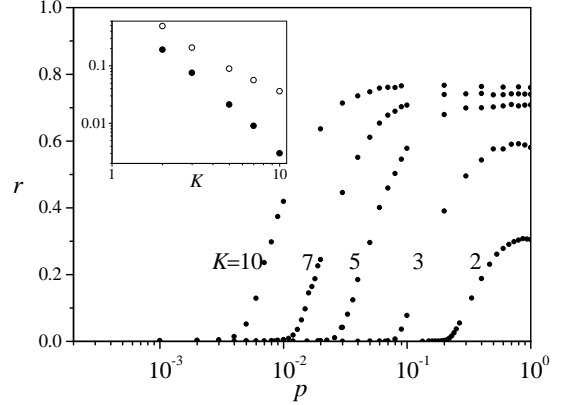


FIG. 4. Average fraction  $r$  of refractory elements at the end of the evolution as a function of the randomness  $p$  for several values of  $K$ , and  $N = 10^5$ . The insert shows the critical randomness  $p_c$  (full dots) and the difference  $r^* - r_1$  (empty dots; see text for definitions of  $r^*$  and  $r_1$ ) as a function of  $K$ .

In summary, our numerical analysis shows that the regimes where the rumor is bounded to a finite neighborhood of the initially infected site and where it affects a finite fraction of the population are separated by a well-defined transition at a finite randomness  $p_c$  of the underlying small-world network. The results of the finite-size scaling analysis support the presence of a critical phenomenon at  $p_c$ . Quite interestingly, the transition is also found if, instead of building a frozen small-world network as above, a dynamic small-world is considered [11]. In this case, each contact of an I-element is established with one of its  $2K$  nearest neighbors with probability  $1 - p$ , and with a randomly chosen site with probability  $p$ . The transition observed for these dynamic small-worlds is of the same type as on static small-world networks, but presents quantitative differences. For  $K = 2$ , for instance, the critical randomness shifts to  $p_c \approx 0.07$ .

The geometrical properties of small-world networks have been shown to exhibit a cross-over from ordered to random behavior at  $p \sim N^{-1}$ , which implies a vanishing critical value of  $p$  for asymptotically large systems [6–8]. In contrast, we have here presented evidence that a dynamical process occurring on such structures exhibits critical behavior at a finite value of the randomness. This difference suggests that an explanation for the origin of the transition in purely geometrical terms is unsuitable,

and specific dynamical properties must be taken into account. Very recently, evidence of critical behavior at finite small-world randomness has been reported for a strictly epidemiological model, whose evolution rules are substantially different from those considered here [12]. In particular, the epidemiological model allows for the transformation  $R \rightarrow S$ , giving rise to a closed disease cycle (SIRS) through recovery. Moreover, the transformation  $I \rightarrow R \rightarrow S$  is fully deterministic. The critical phenomenon found in that case is a transition to global synchronization of local disease cycles, whereas in our propagation process we have a kind of percolation phenomenon [9,10]. In spite of these basic differences, the dependence of the respective order parameters on the randomness  $p$  is strikingly similar, even if compared quantitatively. This similarity calls for further investigation in order to identify and characterize the whole class of small-world dynamical processes with critical behavior at finite randomness, and to give an analytical description of such behavior.

Enlightening discussions with M. Kuperman and G. Abramson are gratefully acknowledged.

*in Statistical Physics* (Springer, Berlin, 1988).

- 
- [1] D. J. Watts and S. H. Strogatz, *Nature* **393**, 440 (1998).
  - [2] D. J. Watts, *Small Worlds* (Princeton University Press, 1999).
  - [3] M. Barthélemy and L. A. N. Amaral, *Phys. Rev. Lett.* **82**, 3180 (1999).
  - [4] M. E. J. Newman and D. J. Watts, *Phys. Lett. A* **263**, 341 (1999).
  - [5] M. E. J. Newman, C. Moore, and D. J. Watts, *Phys. Rev. Lett.* **84**, 3201 (2000).
  - [6] C. F. Moukarzel, *Phys. Rev. E* **60**, R6263 (1999).
  - [7] M. Argollo de Menezes, C. F. Moukarzel, and T. J. P. Penna, *Europhys. Lett.* **50**, 574 (2000).
  - [8] A. Barrat and M. Weigt, *Eur. Phys. J. B* **13**, 547 (2000).
  - [9] M. E. J. Newman and D. J. Watts, *Phys. Rev. E.* **60**, 7332 (1999).
  - [10] C. Moore and M. E. J. Newman, *Phys. Rev. E* **61**, 5678 (2000).
  - [11] S. C. Manrubia, J. Delgado, and B. Luque, *Europhys. Lett.* **53**, 693 (2001).
  - [12] M. Kuperman and G. Abramson, *Phys. Rev. Lett.* **86**, 2909 (2001).
  - [13] D. Maki and M. Thomson, *Mathematical Models and Applications* (Prentice-Hall, Englewood Cliffs, 1973).
  - [14] J. C. Frauenthal, *Mathematical Modelling in Epidemiology* (Springer, Berlin, 1980).
  - [15] J. D. Murray, *Mathematical Biology* (Springer, Berlin, 1989).
  - [16] More precisely, the limit  $r^* = \lim_{N \rightarrow \infty} N_R/N$  for random contacts is the solution to the transcendental equation  $r^* = 1 - \exp(-2r^*)$ .
  - [17] A. Sudbury, *J. Appl. Prob.* **22**, 443 (1985).
  - [18] K. Binder and D. W. Heermann, *Montecarlo Simulation*